

Optics Letters

Measuring the complex orbital angular momentum spectrum of light with a mode-matching method

PENG ZHAO, SHIKANG LI, XUE FENG,* KAIYU CUI, FANG LIU, WEI ZHANG, AND YIDONG HUANG

Department of Electronic Engineering, Tsinghua National Laboratory for Information Science and Technology, Tsinghua University, Beijing 100084, China

*Corresponding author: x-feng@tsinghua.edu.cn

Received 10 January 2017; revised 15 February 2017; accepted 15 February 2017; posted 15 February 2017 (Doc. ID 284420); published 6 March 2017

The relative phase shift among different components in the superposition of orbital angular momentum (OAM) states contains significant information. However, with existing methods of measuring the OAM spectrum, the phase term of the spectrum coefficient is hard to obtain. In this Letter, a mode-matching method is proposed to identify the complex OAM spectrum with a Mach–Zehnder interferometer and a charge-coupled device camera. It has the potential to extend the applications of OAM in scenarios sensitive to the phase factor, for instance, in imaging and quantum manipulation. The method is experimentally demonstrated with the superposition of two or three OAM states, while the maximum deviation of the energy ratio and the relative phase shift is 8.4% and 5.5% of 2π , respectively. © 2017 Optical Society of America

OCIS codes: (050.4865) Optical vortices; (090.2890) Holographic optical elements; (260.6042) Singular optics.

<https://doi.org/10.1364/OL.42.001080>

Since Allen *et al.* elucidated the relationship between the azimuthal phase distribution and the carried orbital angular momentum (OAM) [1], a light beam containing a phase factor of $e^{il\phi}$ is treated as the eigenmode of an OAM state, where ϕ denotes the azimuthal coordinate in a cylindrical coordinate system, and l is an integer named as topological charge or the order of OAM state. In recent years, a light beam carrying OAM attracts more and more research interest within the range from optical communication [2,3], quantum information [4,5], and optical imaging [6] to optical tweezers or spanners [7]. Since any arbitrary light beam can be expressed as the superposition of OAM states, measuring the OAM spectrum possesses remarkable importance for some applications containing more than one OAM state. Several methods have been proposed to measure the OAM spectrum, e.g., counting the spiral fringes [8], diffraction patterns from apertures [9], diffractive holographic filters [10], and optical transformation elements [11]. Nevertheless, the OAM spectrum metrology has not been

well solved, since these aforementioned methods have some deficiencies, including being unable to identify the whole OAM spectrum coefficients simultaneously, being unable to work at the single photon level, and working with very low energy efficiency. Besides the intensity spectrum, it is also important to measure the phase term of the spectrum coefficient. For instance, the relative phase shift between different OAM states can be used to identify the azimuthal direction or arbitrary shape in ghost imaging [6] or form different quantum qubits to realize the quantum memory [12]. Recently, two approaches have been proposed to measure both the power and the phase distribution of the OAM modes simultaneously. In [13] a plasmonic vortex lens is proposed to retrieve OAM distribution of light. This approach offers an integrated scheme to measure hybrid OAM states by one measurement. Furthermore, an OAM complex spectrum analyzer is demonstrated with rotational Doppler effect in [14].

In this Letter, a computational method to measure the complex OAM spectrum is proposed by mode matching. Different from a previous work [13], in which a specially designed component, e.g., plasmonic lens or a rotational reflective object, is required, our method is based on a classical Mach–Zehnder (M–Z) interferometer and a charge-coupled device (CCD). First, a series of pure OAM states is measured with an M–Z interferometer and a CCD camera, and then recorded to serve as expansion bases. Next, the light field under test, which could contain more than one OAM state, is also obtained by the interference patterns in the M–Z interferometer. At last, the OAM spectrum coefficient can be computed from the overlapping integral between the field under test and the recorded OAM basis.

A light beam with the azimuthal phase distribution of $e^{il\phi}$ carries well-defined OAM of $l\hbar$ per photon, where the l is integral number, and the ϕ is the azimuthal coordinate in a cylindrical coordinate (ρ, ϕ, z). Considering the field distribution along the radial coordinate, the electric field of l -order OAM eigenstate can be expressed as

$$E_l(\rho, \phi) = \frac{1}{\lambda} R(k\rho) e^{il\phi}, \quad (1)$$

where $R(k\rho)$ denotes the radial field distribution, while λ and k are the wavelength and wave vector of the light beam, respectively. Without the loss of generality, we assume E_l is normalized by $R(k\rho)$ with a relation of $\int \int E_m(\rho, \phi) E_n^*(\rho, \phi) \rho d\rho d\phi = \delta_{mn}$, where δ_{mn} denotes the Kronecker delta.

Since the fields of all OAM states construct a complete orthogonal base of arbitrary light field, the light field of an arbitrary scalar beam, which is normalized as well, can be expressed as the superposition of OAM states:

$$E = \sum_l m_l E_l, \quad (2)$$

where m_l denotes the weight coefficient of OAM states. It should be noticed that the weight coefficient m_l is a complex number, which is very similar to the Fourier coefficient. The quantity of $|m_l|^2$ would represent the energy ratio of E_l component over the total field, which is often discussed as the OAM intensity spectrum or the energy spectrum, while the phase of m_l contains information as well. The coefficient m_l can be obtained by the integral overlap between E_l component and the total field:

$$m_l = \iint E(\rho, \phi) E_l^*(\rho, \phi) \rho d\rho d\phi. \quad (3)$$

As seen, to obtain the complex OAM spectrum, both electric fields of the light beam under test and the OAM basis states should be known. Hence, we propose a two-step scheme to measure the spectrum with the mode-matching method. The first step, so-called training, is to measure the fields of a series of single OAM state and then record them as the E_l . The second step is to measure the light field of the beam under test denoted as the E and then obtain the coefficient m_l by calculating the overlapping integral with Eq. (3). It can be seen that the phase of the complex OAM spectrum coefficient is defined as the relative phase shift compared with the recorded E_l . In principle, the ambient variations between the two steps, e.g., path delay and beam alignment, would deteriorate the measured results. For the path delay shift, although the absolute value of the measured phase shift is significantly correlated to it, the relative phase shift between different OAM states is relevant since the same extra phase delay is introduced on each OAM state within the light beam under test. Thus, our method is robust to the path delay, and there is no need for stabilizing it. Additionally, due to the same reason, only the relative phase shift between different OAM states is presented in the following section of experimental results. For the beam tilt, it should be well stabilized since the OAM spectrum dispersion would be introduced [15]. In our experiment, we did not observe significant OAM spectrum deviation within the measurement process. Considering the complicated environment of practical application, some stabilizing mechanism may be needed. Actually, we have also proposed a spectrum correction method in [16].

To measure the optical fields, a typical MZ interferometer is employed as shown in Fig. 1. A laser operating at a wavelength of 1550 nm (RIO Orion) and zero-order Gaussian beam is injected into the optical system through a collimator. After that, a half-wave plate (HWP) and a polarizing beam splitter cube (PBS) are used to split the light beam into two paths with orthogonal polarizations and tunable energy ratios. The vertically polarized component would remain the zero-order Gaussian beam and serve as the reference light. In this path,

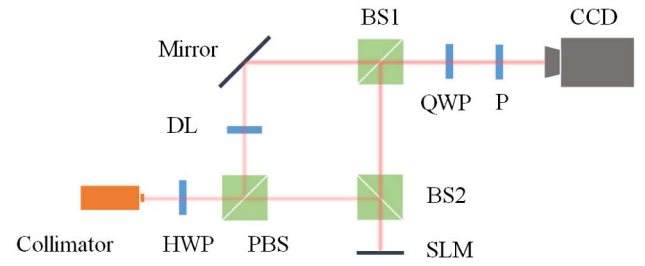


Fig. 1. Scheme of experimental setup. *P*, polarizer; QWP, quarter-wave plate; BS, beam splitter; DL, delay line; PBS, polarizing beam splitter; HWP, half-wave plate; SLM, spatial light modulator.

a delay line (DL) is inserted to control the phase delay. The horizontally polarized component would pass through the PBS, incident to another beam splitter (BS2) and then be reflected toward a spatial light modulator (SLM, PLUTO-TELCO-013), by which several pre-settled OAM states of single or superposed states are generated as the objective beams. The OAM state beams are generated by spiral phase masks, similar to the phase masks in [2]. The reference and objective light beams would interfere at BS1, after which a quarter-wave plate (QWP) and a polarizer (*P*) would filter out the right-hand circularly polarized component of the interfered beam. Finally, a CCD camera connected to a computer would detect and record the interference pattern.

To obtain the complex field distribution of the objective light beam, four intensity patterns of the reference and the objective light beams, as well as their interference pattern, should be measured. We denote the intensity distributions of the objective and reference light beams as I_{obj} and I_{ref} , respectively. Thus, the intensity of the interference (I_{inter}) can be deduced as

$$I_{\text{inter}} = I_{\text{obj}} + I_{\text{ref}} + 2\sqrt{I_{\text{obj}}I_{\text{ref}}}\cos(\varphi_{\text{obj}} - \varphi_{\text{ref}} - \varphi_{\text{del}}), \quad (4)$$

where the φ_{obj} , φ_{ref} , and φ_{del} are the phase distribution of the objective beam, the reference beam, and the extra phase delay in the reference light path, respectively. In principle, two different, but arbitrary, values of φ_{del} are needed to extract the phase distribution of $(\varphi_{\text{obj}} - \varphi_{\text{ref}})$ with the corresponding intensity of the reference beam, objective beam, and interference beam. Here $\varphi_{\text{del}} = 0$ and $\varphi_{\text{del}} = \pi/2$ are selected to achieve the maximum signal-to-noise ratio for calculating the phase distribution. It should be mentioned that an equivalent normalized electric field E_{obj} is adopted to substitute the true field of the objective light beam:

$$E_{\text{obj}}(\rho, \phi) = \frac{\sqrt{I_{\text{obj}}}\rho e^{-i(\varphi_{\text{obj}} - \varphi_{\text{ref}})}}{\iint I_{\text{obj}}\rho d\rho d\phi}. \quad (5)$$

Obviously, there is an extra phase term of $-\varphi_{\text{ref}}$, which is introduced by the light propagation of the reference beam. However, such a term would vanish during the process of calculating the overlapping integral of Eq. (3), since the phase term of reference light beam φ_{ref} is invariable for measuring the OAM basis fields (E_l) and the light field of beam under test (E).

In our experiments, the $-5 \sim 5$ -order OAM state beams are chosen as the bases. For the training step, each single OAM state has been measured with the aforementioned interferometric method. After the complex field of each single state is

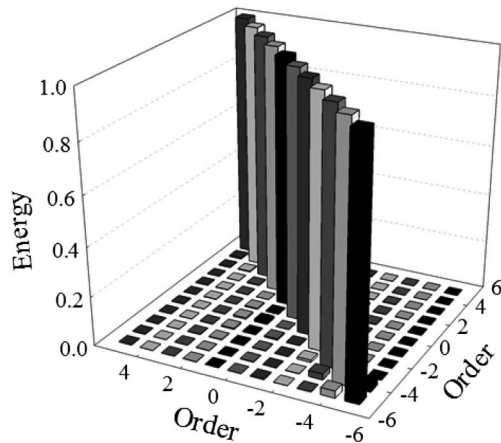


Fig. 2. Overlapping integral of each two from the basis beams with OAM order of $l = -5 \sim 5$.

obtained, the overlapping integral between each two of them has been calculated to verify the mode purity and orthogonality of the OAM bases and Fig. 2 shows the summarized results. The overlapping integral between each OAM basis and itself is normalized as 1. For different OAM states, the largest value of the overlapping integral is 2.88×10^{-2} in our experiment. Although such value is not perfect 0 as the theoretical value, it is small enough to serve as the standard OAM states as reference in the next step.

After the training step, several OAM superposition states are employed to verify our proposed method.

Figures 3(a) and 3(b) show the measured intensity patterns for superposed OAM states consisting of $l = -1$ and $l = 3$ with the same energy ratio of 1:1, but a different relative phase of $\phi_{-1} - \phi_3 = \pi$, 1.5π , where the ϕ_{-1} and ϕ_3 denote the phase factors of the -1 -order and 3 -order states, respectively. The superposed OAM states are generated by segmenting the SLM

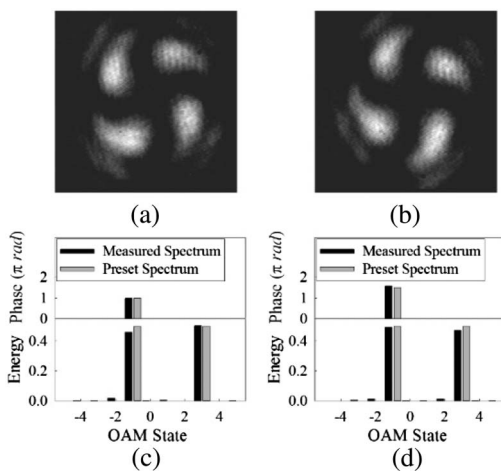


Fig. 3. Measured results of superposition OAM states of $l = -1$ and 3 . (a) and (b) Intensity patterns of the superposed OAM states with the energy ratio of 1:1, but a relative phase shift of $\phi_{-1} - \phi_3 = \pi$ and $\phi_{-1} - \phi_3 = 1.5\pi$. (c) and (d) Preset (gray) and the measured (black) spectra corresponding to the superposed OAM states in (a) and (b).

into several individual parts, while each part produces one single OAM state with a preset phase shift. It could be found that intensity patterns in Figs. 3(a) and 3(b) have similar shapes, but different azimuthal directions, according to the phase shift. With our proposed method, the corresponding complex OAM spectra can be extracted. Figures 3(c) and 3(d) show the obtained OAM spectra corresponding to the light beam in Figs. 3(a) and 3(b). The lower and upper parts of each figure show the intensity spectrum and the relative phase shift. In Figs. 3(c) and 3(d), the gray column is the preset value, while the black column is the measured one. Comparing them, it could be found that the max deviation of the phase measurement is $\sim 3.3\%$ of 2π , while the energy ratio is $\sim 3.8\%$.

As mentioned above, the relative phase shift of two superimposed OAM states determines the different azimuthal direction of the intensity pattern. Specifically, in the case of superposition OAM beams consisting of $l = -1$ and 3 , the intensity patterns are always four rotationally symmetric and bright spots, while the pattern would linearly rotate according to the relative phase shift between the two OAM states. If the relative phase shift changes from 0 to 2π , the pattern would rotate a quarter circumference from the initial position. Thus, the relative phase shift can be identified by the pattern as reported in several previous works [12,17]. Thus, compared with these previous works, our method is not superior for the case of only two superimposed OAM states. However, when more superposed OAM states are involved, the relative phase shifts cannot be simply identified by the intensity pattern, but our method can work to identify the complex OAM spectrum.

Figures 4(a) and 4(b) show the intensity patterns of the superposed OAM states of $l = -1$, 1 , and 3 with the same energy ratio of 1:1:1, but different relative phase shifts. Here the relative phase shift is defined according to OAM state of $l = 3$ as $\Delta\phi_1 = \phi_{-1} - \phi_3$ and $\Delta\phi_2 = \phi_1 - \phi_3$, where the ϕ_{-1} , ϕ_1 , and ϕ_3 denote the OAM spectrum coefficient phase of -1 -order, 1 -order, and 3 -order, respectively. As seen, the patterns show different shapes so that the relative phase shift cannot be

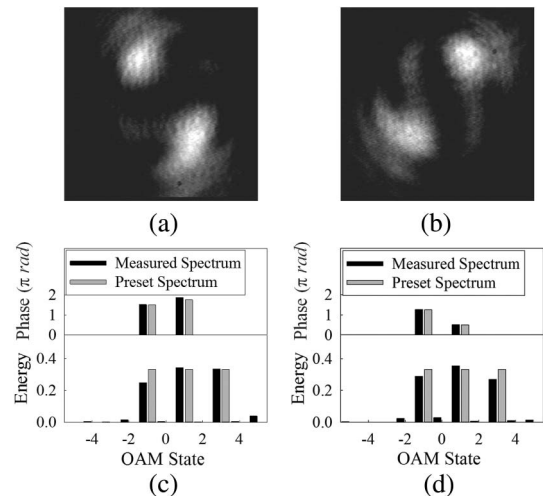


Fig. 4. Measured results of superposition OAM states of $l = -1$, 1 , and 3 . (a) and (b) Intensity patterns of the superposed OAM states with the same energy ratio of 1:1:1, but a different relative phase shift. (c) and (d) Preset (gray) and the measured (black) spectra corresponding to the light beams in (a) and (b).

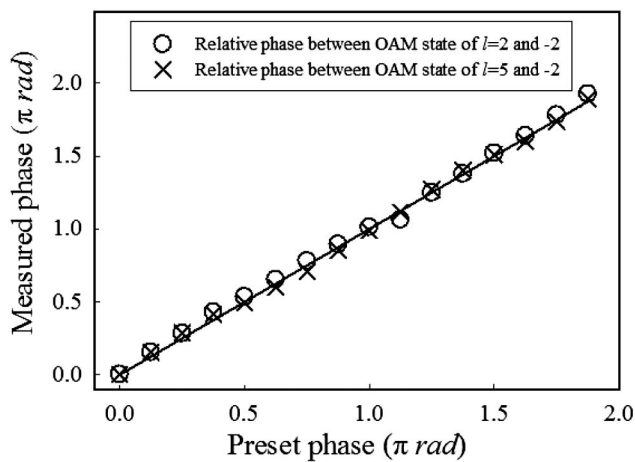


Fig. 5. Measured results of the superposition OAM states of $l = -2, 2,$ and 5 with the energy ratio of 3:2:1. The hollow circle/cross presents the relative phase shift between OAM stats of $l = 2/l = 5$ and that of $l = -2$, respectively, while the straight solid line with a slope of 1 denotes the ideal result.

extracted from the patterns. In Fig. 4(a), the preset values are $\Delta\phi_1 = 1.5\pi$ and $\Delta\phi_2 = 1.75\pi$, while those in Fig. 4(b) are $\Delta\phi_1 = 1.25\pi$ and $\Delta\phi_2 = 0.5\pi$. The lower and upper parts in Figs. 4(c) and 4(d) are the intensity OAM spectral and the relative phase shifts corresponding to the light beam in Figs. 4(a) and 4(b). The relative phase shifts are compared with the phase of 3-order OAM state ϕ_3 as well. The maximum deviation of the measured relative phase and energy ratio are 5.5% of 2π and 8.4%, respectively.

Finally, to evaluate the precision of the phase measurement, a series of experiments has been carried out, and the results are shown in Fig. 5. The results are obtained from the superposed OAM states of $l = -2, 2,$ and 5 with the energy ratio of 3:2:1. In Fig. 5, the solid line shows the ideal result as a straight line with the slope of 1. While the hollow circles/crosses denote the relative phase shift between the state of $l = 2/l = 5$ and that of $l = -2$, respectively. It can be seen that the measured point is quite consistent with the ideal line, and the deviation is about $-4.0\% \sim 0.4\%$ of 2π . This result indicates that our proposed method is reliable to measure the phase shift, and the accuracy is barely relevant to the energy ratio of OAM states.

In this Letter, we have proposed a computational method to identify the complex OAM spectrum by mode matching. With our method, measuring the complex spectrum coefficient has

been experimentally demonstrated with the superposition of two and three OAM states. Specifically, for superposed OAM states of $l = -1, 1,$ and 3 , the maximum deviation of the measured energy ratio and relative phase shift is 8.4% and 5.5% of 2π . Besides the measurement accuracy, it could be noticed that the measurement speed is limited by the response speed of the CCD camera. The performance can be improved by employing a high-speed CCD camera or exploring high-speed photodetector array with a compressed sensing algorithm in the future. We believe that the presented method of measuring a complex OAM spectrum would extend the applications of OAM by the extra information consisting in the relative phase shifts, especially in imaging and quantum manipulation.

Funding. National Science Foundation (NSF) (61621064, 61675112); National Basic Research Program of China (2013CB328704).

REFERENCES

1. L. Allen, M. W. Beijersbergen, R. J. C. Spreeuw, and J. P. Woerdman, *Phys. Rev. A* **45**, 8185 (1992).
2. J. Wang, J.-Y. Yang, I. M. Fazal, N. Ahmed, Y. Yan, H. Huang, Y. Ren, Y. Yue, S. Dolinar, M. Tur, and A. E. Willner, *Nat. Photonics* **6**, 488 (2012).
3. D. Zhang, X. Feng, and Y. Huang, *Opt. Express* **20**, 26986 (2012).
4. S. Straupe and S. Kulik, *Nat. Photonics* **4**, 585 (2010).
5. A. C. Dada, J. Leach, G. S. Buller, M. J. Padgett, and E. Andersson, *Nat. Phys.* **7**, 677 (2011).
6. N. Uribe-Patarroyo, A. Fraine, D. S. Simon, O. Minaeva, and A. V. Sergienko, *Phys. Rev. Lett.* **110**, 43601 (2013).
7. A. T. O’Neil and M. J. Padgett, *Opt. Commun.* **193**, 45 (2001).
8. M. Padgett, *Am. J. Phys.* **64**, 77 (1996).
9. J. M. Hickmann, E. J. S. Fonseca, W. C. Soares, and S. Chávez-Cerda, *Phys. Rev. Lett.* **105**, 053904 (2010).
10. A. Mair, A. Vaziri, G. Weihs, and A. Zeilinger, *Nature* **412**, 313 (2001).
11. M. P. Lavery, G. C. Berkhout, J. Courtial, and M. J. Padgett, *J. Opt.* **13**, 64006 (2011).
12. A. Nicolas, L. Veissier, L. Giner, E. Giacobino, D. Maxein, and J. Laurat, *Nat. Photonics* **8**, 234 (2014).
13. H. Zhou, J. Dong, J. Zhang, and X. Zhang, *Sci. Rep.* **6**, 27265 (2016).
14. H. Zhou, D. Fu, J. Dong, P. Zhang, D. Chen, X. Cai, F. Li, and X. Zhang, “Orbital angular momentum complex spectrum analyzer for vortex light based on rotational Doppler effect,” arXiv: 160900567 (2016).
15. M. V. Vasnetsov, V. A. Pas’ko, and M. S. Soskin, *New J. Phys.* **7**, 46 (2005).
16. P. Zhao, S. Li, Y. Wang, K. Cui, F. Liu, W. Zhang, and Y. Huang, *Sci. Rep. SREP-16-45087* (submitted for publication).
17. A. Vaziri, G. Weihs, and A. Zeilinger, *J. Opt. B* **4**, S47 (2002).